

# Gel-sol evolution of cyclodextrin-based nanosponges: role of the macrocycle size

F. Castiglione · V. Crupi · D. Majolino ·  
A. Mele · L. Melone · W. Panzeri · C. Punta ·  
B. Rossi · F. Trotta · V. Venuti

Received: 15 November 2013 / Accepted: 4 February 2014 / Published online: 14 February 2014

F. Castiglione · A. Mele · L. Melone · C. Punta  
Department of Chemistry, Materials and Chemical Engineering  
“G. Natta”, Politecnico di Milano, Piazza L. Da Vinci 32,  
20133 Milan, Italy

V. Crupi · D. Majolino · V. Venuti  
Department of Physics and Earth Sciences, University of  
Messina, Viale Ferdinando Stagno D’Alcontres 31,  
98166 Messina, Italy

A. Mele · W. Panzeri  
CNR-Institute of Chemistry of Molecular Recognition, via L.  
Mancinelli, 720131 Milan, Italy

C. Punta  
INSTM Local Unit, Politecnico di Milano, Milan, Italy

B. Rossi (✉)  
Department of Physics, University of Trento, via Sommarive 14,  
38123 Povo Trento, Italy  
e-mail: rossi@science.unitn.it

B. Rossi  
INSTM Local Unit, University of Trento, Trento, Italy

F. Trotta  
Department of Chemistry, University of Torino, Via Pietro  
Giuria 7, 10125 Turin, Italy

## Introduction

Hydrogels are soft materials with very intriguing properties [1–3] and they find important uses of high-social impact, such as in the field of tissue engineering and controlled drug delivery [4–8]. For example, hydrogels have been used as localized drug depots [9–11] because they are hydrophilic and biocompatible and their drug release rates can be triggered [12] by interactions with biomolecular stimuli [13, 14]. In this sense, the drug kinetic profile of these systems can be effectively engineered according to the desired drug release schedule, by tuning swelling, cross-linking density, and degradation rate. Another common use of hydrogels arises from their suitability as scaffold materials: widely studied applications are for cartilage, central nervous system, and spinal cord injury

repair strategies [14, 15]. The mild gelling conditions and in situ polymerization capabilities of hydrogels enable the simultaneous inclusion of cells and drugs. This permits the incorporation of both specific drugs for cell-supporting and also active molecules for local delivery into the target tissue [3, 7]. Again, a thixotropic behaviour of the hydrogels is noteworthy, as it allows not only injectability, but also local persistence of gel once placed in situ.

The knowledge of drug release mechanisms occurring in hydrogel systems plays a key-role in the design of smart system for bio-life technological fields, like tissue engineering, cell therapy or drug delivery. From the other hand, a deeper understanding of these phenomena is a challenging task because a thorough physico-chemical and structural characterization of hydrogel matrix is sometimes missing.

In particular, it would be widely desirable that hydrogels could be as much as possible stimuli-responsive, and hence able to modify their structural properties or undergo phase transitions in a controlled way, i.e. by changing temperature and/or pH, as examples.

In this frame, the hydrogels obtained by the swelling cyclodextrin nanosponges (CDNS) seems to be good candidates as stimuli-responsive systems for the entrapment and release of bio-active compounds. As previously demonstrated on paradigmatic CDNS [16] gel to liquid suspension evolution can be induced by simply changing the hydration level of the system.

A wide investigation of the structural and dynamical properties, at molecular level, of cyclodextrin nanosponges in dry state have been recently performed by a variety of experimental techniques and numerical methods [16–22]. All the results pointed out that reticulation, rigidity and swelling properties of CDNS can be efficiently modulated by suitable choice of the cross-linking agent or the cross-linker/cyclodextrin molar ratio  $n$ .

More recently [23], a through inspection of the vibrational dynamics of  $\beta$ -cyclodextrin-based hydrogels, performed by Fourier transform infrared absorption in attenuated total reflectance geometry (FTIR-ATR) and Raman spectroscopies, shed light on the complex interplay between physical and chemical interactions which yield the formation and stabilization of the hydrogel network. It was found that, on one side, the aggregation of nanosized CDNS domains over the macroscopic length scale of the gel is driven by the establishment of inter- and intramolecular hydrogen bonds involving water molecules and/or the hydroxyl groups of CDNS (CDNS can swell because of the progressive penetration of water molecules inside the hydrophilic pores of the polymer and, at the same time, different CDNS domains can aggregate via non-covalent interactions with each other), and, on the other hand, the

the covalent cross-linking degree of the polymer. Again, a direct evidence of a gel to liquid evolution in  $\beta$ -cyclodextrin-based hydrogels was given by FTIR-ATR measurements [24], that allowed us to monitor the changes in the vibrational dynamics of the system by accounting the connectivity pattern of water molecules, involved and not involved in hydrogen bonds tetrahedral arrangements, concurring to the gelation process. As main result, a characteristic cross-over hydration level  $h_{cross}$  was experimentally determined, above which the water tetrahedral arrangements become dominant. It has been correlated to the other parameters of the system, such as the absorption ability of CDNS and the elasticity of the polymeric matrix, and proved to be, once again, strongly dependent on the molar ratio  $n$ .

These findings suggested the existence of a diagram of the CDNS hydrogels, in which the molar ratio  $n$  seems to play a key-role in defining the nano- and macroscopic properties of the system.

However, it should be stressed that all the investigations so far carried out mainly focused on the role of the cross-linking agent and water content. In principle, also the carbohydrate part is expected to influence the overall properties of the nanosponge. In particular, the macrocycle size of starting cyclodextrins is still an unexplored parameter in the nanosponge characterization. Additionally, it is still unknown whether or not the macroring plays a role in defining the physical and absorption properties of CDNS. Thus, comparative experiments on cyclodextrins and homologous linear oligomers of amylose—e.g. linear maltoheptaose versus  $\beta$ -cyclodextrin—are currently in progress.

As a starting point of the investigation of the ring properties on the behaviour of CDNS, we present here a detailed FTIR-ATR investigation of the spectral changes occurring in the O–H profile of water molecules confined in CDNS obtained from  $\alpha$ -CD and an activated derivative of ethylenediaminetetraacetic acid (EDTA), at different EDTA/ $\alpha$ -CD molar ratio. These results corroborate the reliability of the spectroscopic approach as a powerful tool to investigate the crucial role played by water in the evolution of nanosponges hydrogel.

## Experimental methods

### Chemicals

The nanosponges were obtained following the synthetic procedure previously reported [25–27].

In order to obtain  $\alpha$ -CDEDTA $1n$  nanosponges, anhydrous  $\alpha$ -CD was dissolved at room temperature in anhydrous DMSO containing anhydrous  $\text{Et}_3\text{N}$ . Then, the cross-

linking agent ethylenediaminetetraacetic acid (EDTA) dianhydride was added at molecular ratios of 1: $n$  (with  $n = 2, 6, 10$ ) under intense magnetic stirring. The polymerization was complete in few minutes obtaining a solid that was broken up with a spatula and washed with acetone in a Soxhlet apparatus for 24 h. The pale yellow solid was finally dried under vacuum.

The corresponding hydrogel of nanosponges were prepared by adding the dry samples of  $\alpha$ -CDEDTA1 $n$  ( $n = 2, 6, 10$ ) of suitable amount of double-distilled water (Sigma) in order to obtain different levels of hydration  $h$  in the range  $2 \div 25.5$ . The hydration level  $h$  is defined as weight ratio  $H_2O/\alpha$ -CDEDTA1 $n$ .

All the gel samples were freshly prepared and used for FTIR-ATR measurements.

### FTIR-ATR measurements

FTIR-ATR measurements were performed by means of a BOMEM DA8 Fourier transform spectrometer, using a Globar source, a KBr beamsplitter, and a thermo-electrically cooled deuterated triglycene sulphate (DTGS) detector. Spectra were collected at room temperature in the  $400 \div 4,000 \text{ cm}^{-1}$  wavenumber range. Samples were contained in a Golden Gate diamond ATR system, based on the attenuated total reflectance (ATR) technique [28]. Each spectrum was recorded in dry atmosphere, in order to avoid dirty contributions, with a resolution of  $4 \text{ cm}^{-1}$ , and is an average of 100 repetitive scans, so guaranteeing a good signal-to-noise ratio and high reproducibility. No mathematical correction (e.g. smoothing) was done, and spectroscopic manipulation such as baseline adjustment and normalization were performed using the Spectralcalc software package GRAMS (Galactic Industries, Salem, NH, USA). Band decomposition of the O–H stretching spectral range ( $2,800 \div 3,800 \text{ cm}^{-1}$ ) was undertaken using the curve fitting routine provided in the PeakFit 4.0 software package, which enabled the type of fitting function to be selected. The strategy adopted was to use well-defined shape components of Voigt functions with all the parameters allowed to vary upon iteration. The statistical parameters were used as a guide to ‘best fit’ characterized by  $r^2 = 0.9999$  for all the investigated systems.

### Results and discussion

In Figure 1(a)–(b) we report the high-frequency FTIR-ATR spectra of  $\alpha$ -CDEDTA12 and  $\alpha$ -CDEDTA16 hydrogels, respectively, prepared at different levels of hydration  $h$ , i.e.  $h = 2.5$  and  $h = 25.5$ . In this spectral range, we can recognize the typical O–H stretching vibration of water, particularly sensitive to the geometrical arrangement of the

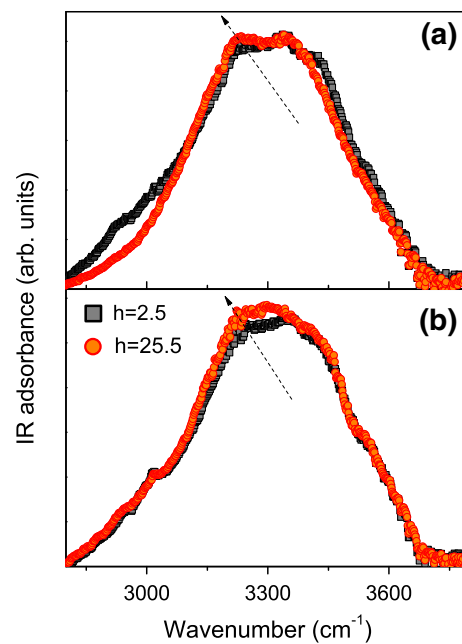


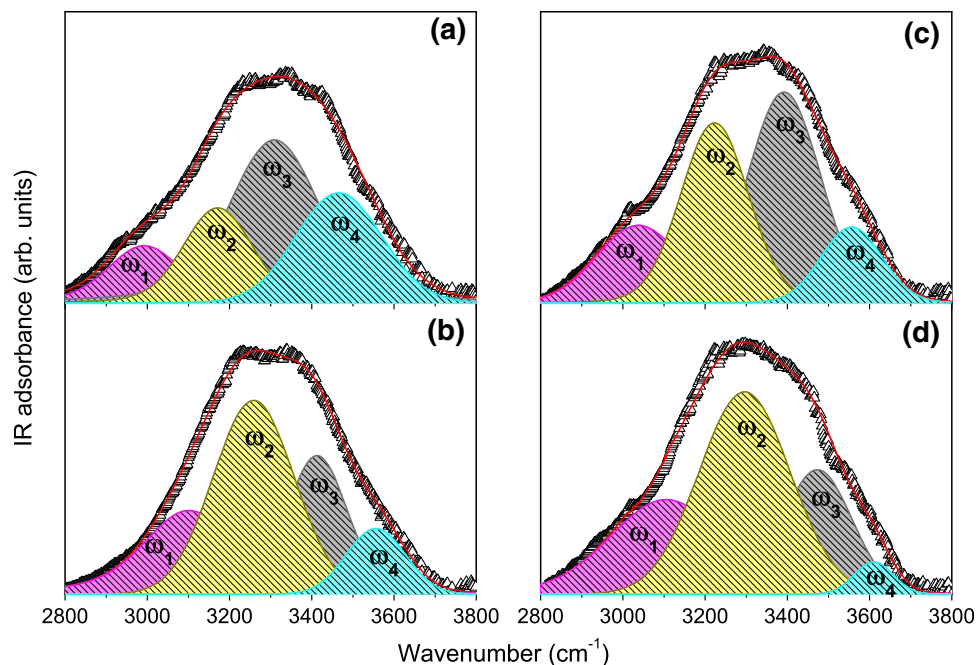
**Fig. 1** Experimental FTIR-ATR spectra in the O–H stretching region for  $\alpha$ -CDEDTA12 (a) and  $\alpha$ -CDEDTA16 (b) hydrogels at  $h = 2.5$  (black closed squares) and  $h = 25.5$  (red open circles). (Color figure online)

hydrogen bond network involving the  $H_2O$  molecules entrapped in the pores of the CDNS hydrogel. The spectra have been normalized with respect to the high-frequency shoulder in order to better put into evidence the modifications induced by variations in the hydration level.

The spectra of Fig. 1 show that the O–H stretching band is sensitive to the hydration level of the system. In particular, for all the investigated hydrogels, low-frequency contributions increase with respect to the high-energy one, by increasing  $h$ . These findings are consistent with what already observed on  $\beta$ -CD-based nanosponges hydrogels prepared with EDTA [24] or on water confined in a variety of nanoporous matrices [29, 30]. They are interpreted in terms of an enhancement of the population of  $H_2O$  molecules strongly interconnected in a highly cooperative H-bond network.

A more quantitative picture can be obtained by the decomposition method successfully used and described previously [29, 30]. The O–H stretching vibration is decomposed into sub-bands, describing classes of O–H oscillators corresponding to transient H-bonded and non H-bonded structures [31, 32]. By looking at the minima in the second derivative profile of the O–H stretching region, that approximately correspond to the maxima for the band components, four contributions can be isolated and the related centre-frequencies can be determined. The curve fitting procedures, by using Voigt functions, were applied to the experimental profiles based on these wavenumber values.

**Fig. 2** Examples of spectral decomposition of O–H stretching profile for  $\alpha$ -CDEDTA12 at  $h = 2.5$  (a) and  $h = 25.5$  (b), and for  $\alpha$ -CDEDTA16 at  $h = 2.5$  (c) and  $h = 25.5$  (d) hydrogels. The experimental data (*open up triangles*) are reported together with the best-fit (*red line*) and the decomposition components. (Color figure online)



In particular, the two lowest wavenumber sub-bands,  $\omega_1$  and  $\omega_2$ , respectively describe the symmetric and asymmetric O–H stretching mode of water molecules involved in tetrahedral environments exhibiting strong H-bond on both the hydrogen atoms. The third contribution,  $\omega_3$ , has been assigned to the non-in-phase O–H stretching vibration of tetrahedral environments linked by “bifurcated” H-bonds, giving rise to distorted structures. Finally, the sub-band at the highest energy,  $\omega_4$ , takes into account the O–H mode of those water molecules for which the hydrogen bond network is, totally or at least partially, destroyed.

As an example, the results of the best fitting procedure applied to  $\alpha$ -CDEDTA12 at  $h = 2.5$  (a) and  $h = 25.5$  (b), and for  $\alpha$ -CDEDTA16 at  $h = 2.5$  (c) and  $h = 25.5$  (d) hydrogels are shown in Fig. 2.

The percentage intensities of the components are representative of the different populations of the particular species assigned to each component [33, 34]. In Fig. 3 their behaviour as a function of  $h$  is reported for all the investigated samples.

By increasing the level of hydration of the hydrogel, an enhancement of the population of bulk-like tetrahedral environments with respect to non bulk-like H<sub>2</sub>O molecules appears immediately evident. This finding provides a quantitative base for the changes in the hydrogen bonding scheme qualitatively hypothesized by the aforementioned description of the experimental FTIR-ATR spectra. We can then retain the obtained results are model-independent.

The sums of the intensities ( $I_1 + I_2$ ) and ( $I_3 + I_4$ ) are related to the bulk-like and non bulk-like populations of water molecules, respectively. The plot of ( $I_1 + I_2$ ) and

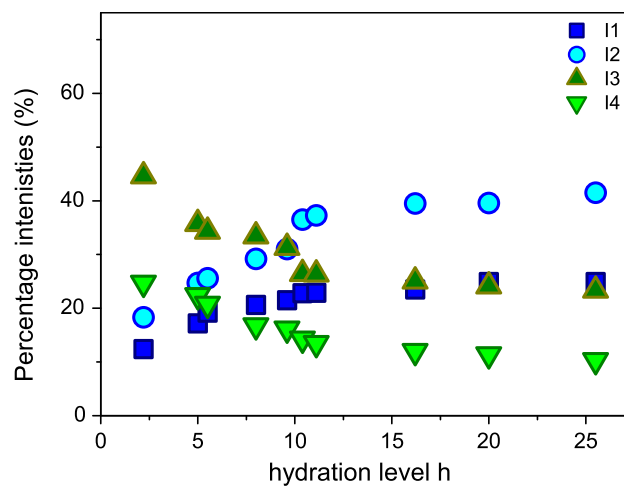


**Fig. 3** Percentage intensities  $I_i$  of the different spectral contributions to the O–H stretching band as a function of the hydration level  $h$  for  $\alpha$ -CDEDTA12 hydrogel.  $I_1$ : closed squares,  $I_2$ : closed circles,  $I_3$ : closed up triangles,  $I_4$ : closed down triangles

( $I_3 + I_4$ ) as a function of  $h$  is reported in Fig. 4(a)–(b) for  $\alpha$ -CDEDTA12 and  $\alpha$ -CDEDTA16 hydrogels, respectively. For both contributions, the curves show a saturation behaviour with increasing  $h$ . As a matter of fact, the balance of the bulk-like and non bulk-like H<sub>2</sub>O molecules populations is well described by a logistic sigmoid function. The experimental curves indicate that, with increasing the hydration level, the system tends to settle on a situation in which H<sub>2</sub>O molecules involved in tetrahedral H-bonded network become by far predominant with respect to water molecules arranged in patterns having a connectivity degree less than four.

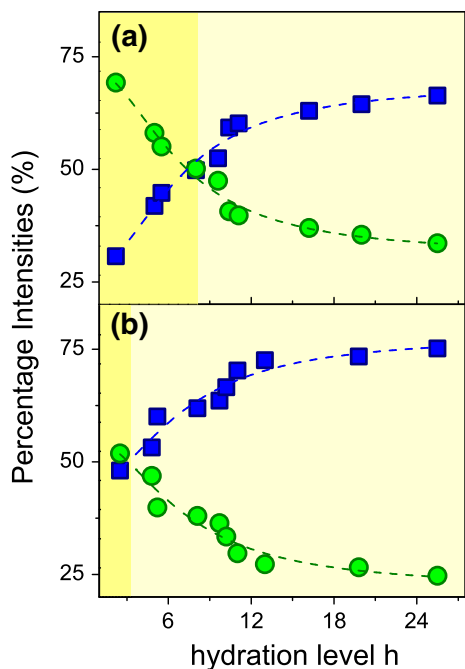


**Fig. 4** Percentage intensities  $I_1 + I_2$  (closed squares) and  $I_3 + I_4$  (closed circles) of the spectral contributions to the O–H stretching band, as a function of the hydration  $h$ , for (a)  $\alpha$ -CDEDTA12 and (b)  $\alpha$ -CDEDTA16

A simple model accounting for the experimental curves can be formulated in terms of saturation of CDNS sites capable to entrap water molecules. Consequently, for any further increase of the hydration level, the excess water molecules will not be absorbed by the CDNS pores, and will tend to develop tetrahedral arrangements similar to those exhibited in the bulk phase. Furthermore, the plots in Fig. 4 point out the cross-over point between the two different contributions at a specific hydration level, here referred to as  $h_{cross}$ . The value of  $h_{cross}$  defines two different hydration regions, evidenced in Fig. 4, where different states can be observed. The system appears as a rigid gel for  $h < h_{cross}$ , and as a fluid suspension for  $h > h_{cross}$ . Then, as already concluded for the  $\beta$ -CDNS hydrogels prepared with EDTA [24],  $h_{cross}$  constitutes a key parameter of the gel-to-sol evolution observed for these systems.

In Fig. 5 we report the critical mass ratios  $m$  determined for  $\alpha$ - and  $\beta$ -CDEDTA nanosponges (in the case of  $\beta$ -CDEDTA samples data are extracted from Ref. [24]) corresponding to the gelation point. Mass ratios  $m$  are defined as  $m = \text{mass of CDNS}/\text{mass of H}_2\text{O} = 1/h$ .

The plots of Fig. 5 indicate that  $m$  at gelation point changes by varying  $n$ , showing a maximum for  $n = 6$ . It was already demonstrated for dry  $\beta$ -CDNS [16–24] that a 6-fold excess of cross-linker with respect to CD corresponds to the maximum extent of bond connectivity and stiffness of the polymer. On the other side, for hydrated  $\beta$ -

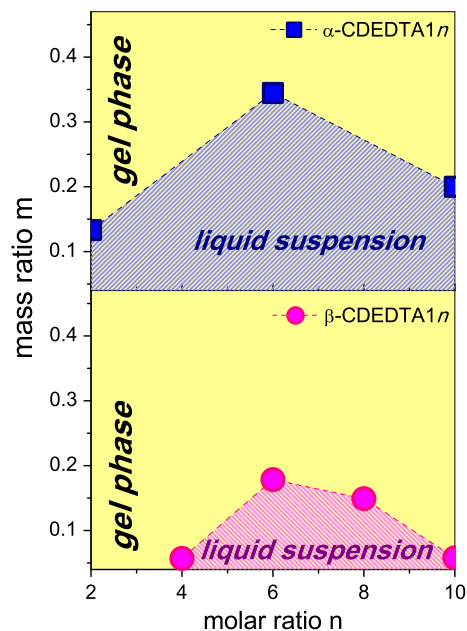


**Fig. 5** Critical mass ratios  $m$  corresponding to the gelation point estimated for  $\alpha$ -CDEDTA1n (top panel) and  $\beta$ -CDEDTA1n (bottom panel) hydrogels as a function of the parameter  $n$

CDNS [24],  $n = 6$  coincides also with the formation of the most strongly interconnected hydrogen-bonded network in the hydrogel. Further excess of cross-linking agent provided, for dry systems, branching of  $\beta$ -CD units rather than further reticulation and, for hydrogels, a reduction of the connectivity degree of the H-bond scheme due to an increased steric hindrance of the polymeric network. The maximum found at  $n = 6$  also for  $\alpha$ -CDEDTA nanosponges confirms that the properties observed at this molar ratio in ester-based dry and hydrated CDNS are deeply related to the structure of the polymer network as obtained by the synthetic process. Again, in good agreement with what previously observed for  $\beta$ -CDEDTA nanosponges (Fig. 5), also  $\alpha$ -CDEDTA16 nanosponge is able to entrap much less water with respect to  $\alpha$ -CDEDTA12 and  $\alpha$ -CDEDTA110 samples (Fig. 5). Coherently,  $\alpha$ -CDEDTA12 nanosponge appears to be the most absorbent one. Explanations to this occurrence were previously ascribed [24] to an interplay between higher rigidity and reduced dimensions of the pores of the network of these systems at  $n = 6$ . We are currently further investigating these hypotheses by a small angle neutron scattering analysis.

Interestingly, if  $n$  is kept fixed, higher  $m$ -values are obtained in the case of  $\alpha$ - with respect to  $\beta$ -CD, as clearly shown in the diagrams of Fig. 5, according to the fact that, namely,  $\alpha$ -CDEDTA exhibit lower swelling properties with respect to  $\beta$ -CDEDTA. The use of  $\alpha$ -CD instead of  $\beta$ -CD as starting material for the polycondensation clearly allows for a modulation of the stability range of the liquid

suspension and gel states, thus adding further elements of versatility to these systems in view of possible applications.

## Conclusions

$\alpha$ -cyclodextrin based nanosponges have been progressively hydrated in order to follow the evolution from rigid gel to liquid suspension, monitoring at the same time the spectral modifications occurring in the O–H stretching vibrational profile of water molecules as revealed by Fourier transform infrared spectroscopy in attenuated total reflectance geometry (FTIR-ATR). The use of decomposition and best-fitting procedures allowed us to recognize different classes of oscillators contributing to the O–H band, involved in hydrogen bonded transient structures with different degree of co-operativity.

From the results, tetrahedral H<sub>2</sub>O environments are proved to be favoured by the increasing of the hydration level, and their contribution become predominant once a cross over hydration level  $h_{cross}$  is reached. A comparison of the diagrams obtained for homologous CDNS prepared from  $\alpha$ - and  $\beta$ -CD shows how the macrocycle dimension allows to modulate the gelation points at constant CD/crosslinker molar ratio  $n$ . This finding is likely to be exploited for the design of suitable stimuli-responsive systems.

## References

1. Hoare, T.R., Kohane, D.S.: Hydrogels in drug delivery: progress and challenges. *Polymer* **49**, 1993–2007 (2008)
2. Lin, C.C., Metters, A.T.: Hydrogels in controlled release formulations: network design and mathematical modeling. *Adv. Drug Delivery Rev.* **58**, 1379–1408 (2006)
3. Slaughter, B.V., Khurshid, S.S., Fisher, O.Z., Khademhosseini, A., Peppas, N.A.: Hydrogels in regenerative medicine. *Adv. Mater.* **21**, 3307–3329 (2009)
4. Baumann, M.D., Kang, C.E., Stanwick, J.C., Wang, Y.F., Kim, H., Lapitsky, Y., Shoichet, M.S.: An injectable drug delivery platform for sustained combination therapy. *J. Controlled Release* **138**, 205–213 (2009)
5. Kim, Y.T., Caldwell, J.M., Bellamkonda, R.V.: Nanoparticle-mediated local delivery of methylprednisolone after spinal cord injury. *Biomaterials* **30**, 2582–2590 (2009)
6. Baumann, M.D., Kang, C.E., Tator, C.H., Shoichet, M.S.: Intrathecal delivery of a polymeric nanocomposite hydrogel after spinal cord injury. *Biomaterials* **31**, 7631–7639 (2010)
7. Santoro, M., Marchetti, P., Rossi, F., Perale, G., Castiglione, F., Mele, A., Masi, M.: Smart approach to evaluate drug diffusivity in injectable agar-Carbomer hydrogels for drug delivery. *J. Phys. Chem. B* **115**, 2503–2510 (2011)
8. Rossi, F., Casalini, T., Santoro, M., Mele, A., Perale, G.: Methylprednisolone release from agar-Carbomer-based hydrogel: a promising tool for local drug delivery. *Chem. Pap.* **65**, 903–908 (2011)
9. Gagnon, M.A., Lafleur, M.: Self-diffusion and mutual diffusion of small molecules in high-set curdlan hydrogels studied by <sup>31</sup>P NMR. *J. Phys. Chem. B* **113**, 9084–9091 (2009)
10. Brandl, F., Kastner, F., Gschwind, R.M., Blunk, T., Tessmar, J., Gopferich, A.: Hydrogel-based drug delivery systems: comparison of drug diffusivity and release kinetics. *J. Controlled Release* **142**, 221–228 (2010)
11. Lin, C.C., Boyer, P.D., Aimetti, A.A., Anseth, K.S.: Regulating MCP-1 diffusion in affinity hydrogels for enhancing immunoisolation. *J. Control Release* **142**, 384–391 (2010)
12. Biondi, M., Ungaro, F., Quaglia, F., Netti, P.A.: Controlled drug delivery in tissue engineering. *Adv. Drug Delivery Rev.* **60**, 229–242 (2008)
13. Peppas, N.A., Hilt, J.Z., Khademhosseini, A., Langer, R.: Hydrogels in biology and medicine: from molecular principles to bionanotechnology. *Adv. Mater.* **18**, 1345–1360 (2006)
14. Elisseff, J., McIntosh, W., Anseth, K., Riley, S., Ragan, P., Langer, R.: Photoencapsulation of chondrocytes in poly(ethylene oxide)-based semi-interpenetrating networks. *Biomed. Mater. Res.* **51**, 164–171 (2000)
15. Rossi, F., Perale, G., Masi, M.: Biological buffered saline solution as solvent in agar-Carbomer hydrogel synthesis. *Chem. Pap.* **64**, 573–578 (2010)
16. Mele, A., Castiglione, F., Malpezzi, L., Ganazzoli, F., Raffaini, G., Trotta, F., Rossi, B., Fontana, A.: HR MAS NMR, powder XRD and Raman spectroscopy study of inclusion phenomena in  $\beta$ -CD nanosponges. *J. Incl. Phenom. Macrocycl. Chem.* **69**, 403–409 (2011)
17. Castiglione, F., Crupi, V., Majolino, D., Mele, A., Rossi, B., Trotta, F., Venuti, V.: Inside new materials: an experimental numerical approach for the structural elucidation of nanoporous cross-linked polymers. *J. Phys. Chem. B* **116**, 13133–13140 (2012)
18. Rossi, B., Caponi, S., Castiglione, F., Corezzi, S., Fontana, A., Giarola, M., Mariotto, G., Mele, A., Petrillo, C., Trotta, F., Viliani, G.: Networking properties of cross-linked polymeric systems probed by inelastic light scattering experiments. *J. Phys. Chem. B* **116**, 5323–5327 (2012)
19. Castiglione, F., Crupi, V., Majolino, D., Mele, A., Panzeri, W., Rossi, B., Trotta, F., Venuti, V.: Vibrational dynamics and hydrogen bond properties of beta-CD nanosponges: an FTIR-ATR, Raman and solid-state NMR spectroscopic study. *J. Incl. Phenom. Macrocycl. Chem.* **75**, 247–254 (2013)
20. Castiglione, F., Crupi, V., Majolino, D., Mele, A., Rossi, B., Trotta, F., Venuti, V.: Effect of cross-linking properties on the vibrational dynamics of cyclodextrin-based polymers: an experimental-numerical study. *J. Phys. Chem. B* **116**, 7952–7958 (2012)
21. Crupi, V., Fontana, A., Giarola, M., Majolino, D., Mariotto, G., Mele, A., Melone, L., Punta, C., Rossi, B., Trotta, F., Venuti, V.: Connection between the vibrational dynamics and the cross-linking properties in cyclodextrin-based polymers. *J. Raman Spectrosc.* **44**, 1457–1462 (2013)
22. Castiglione, F., Crupi, V., Majolino, D., Mele, A., Rossi, B., Trotta, F., Venuti, V.: Vibrational spectroscopy investigation of swelling phenomena in cyclodextrin nanosponges. *J. Raman Spectrosc.* **44**, 1463–1469 (2013)
23. Crupi, V., Majolino, D., Mele, A., Rossi, B., Trotta, F., Venuti, V.: Modelling the interplay between covalent and physical interactions in cyclodextrin-based hydrogel: effect of water confinement. *Soft Matter* **9**, 6457–6464 (2013)
24. Crupi, V., Majolino, D., Mele, A., Melone, L., Punta, C., Rossi, B., Toraldo, F., Trotta, F., Venuti, V.: Direct evidence of gel-sol evolution in cyclodextrin-based hydrogel as revealed by FTIR-ATR spectroscopy. *Soft Matter* (2014). doi:[10.1039/C3SM52354C](https://doi.org/10.1039/C3SM52354C)

25. Trotta, F., Tumiatti, W. 2003 Cross-linked polymers based on cyclodextrin for removing polluting agents; Patent WO 03/085002
26. Trotta, F., Tumiatti, W., Cavalli, R., Zerbinati, O., Roggero, C.M., Vallero, R. 2006 Ultrasound-assisted synthesis of cyclodextrin-based nanosponges; Patent number WO 06/002814
27. Trotta, F., Tumiatti, W., Cavalli, R., Roggero, C., Mognetti, B., Berta, G. 2009 Cyclodextrin-based nanosponges as a vehicle for antitumoral drugs; Patent number WO 09/003656 A1
28. Crupi, V., Longo, F., Majolino, D., Venuti, V.: Vibrational properties of water molecules adsorbed in different zeolitic frameworks. *J. Phys. Condens. Matt.* **18**, 3563–3580 (2006)
29. Crupi, V., Majolino, D., Migliardo, P., Venuti, V.: Diffusive relaxations and vibrational properties of water and H-bonded systems in confined state by neutrons and light scattering: state of the art. *J. Phys. Chem. B* **104**, 11000–11012 (2000)
30. Crupi, V., Majolino, D., Migliardo, P., Venuti, V.: Wanderlingh: a FT-IR absorption analysis of vibrational properties of water encaged in NaA zeolites: evidence of a “structure maker” role of zeolitic surface. *Eur. Phys. J. E* **12**, S55–S58 (2003)
31. Crupi, V., Interdonato, S., Longo, F., Majolino, D., Migliardo, P., Venuti, V.: New insight on the hydrogen bonding structures of nanoconfined water: a Raman study. *J. Raman Spectrosc.* **39**, 244–249 (2008)
32. Crupi, V., Longo, F., Majolino, D., Venuti, V.: Raman spectroscopy: probing dynamics of water molecules confined in nanoporous silica glasses. *Eur. Phys. J. Special Topics* **141**, 61–64 (2007)
33. Crupi, V., Majolino, D., Migliardo, P., Venuti, V.: Inter- and intramolecular hydrogen bond in liquid polymers: a Fourier transform infrared response. *Mol. Phys.* **98**, 1589–1594 (2000)
34. Crupi, V., Longo, F., Majolino, D., Venuti, V.: T dependence of vibrational dynamics of water in ion-exchanged zeolites A: a detailed Fourier transform infrared attenuated total reflection study. *J. Chem. Phys.* **123**, 154702 (2005)